

Dušan Ćurčija, Ilija Mamuzić, Marian Buršak, Jiri Klíber

ISSN 0350-350X

GOMABN 51, 2, 123-147

Izvorni znanstveni rad / Original scientific paper

EFFECTS OF CROSS-ROUGHNESS ON COLD ROLLING PROCESS WITH GREASES

Abstract

The article presents the formulas for calculating the grease layer height at inlet dia of deformation zone, depending on cross-roughness of the rolls and the strip. Analytical solutions covering the fields of all gripping angles of cold rolling process take into account the effect of the grease layer height on the strip in front of the rolls. Explanations are offered on how to calculate the grease layer height when roughness can be neglected, i.e. when it reaches an ideal smooth surface, and when the grease layer height on the strip in front of the rolls can be neglected.

The formulas relating to the laminar flow of grease and isothermic conditions of cold rolling process seem to be unique, as far as data from literature are concerned.

1. Introduction

For the situation involving smooth surfaces of the rollers and the strip, the mathematical description is provided by the differential equation (1):

$$\frac{dp}{dx} = \frac{6\mu(v_0 + v_R)}{\varepsilon^2(x)} - \frac{12\mu Q}{\varepsilon^3(x)} \quad (1)$$

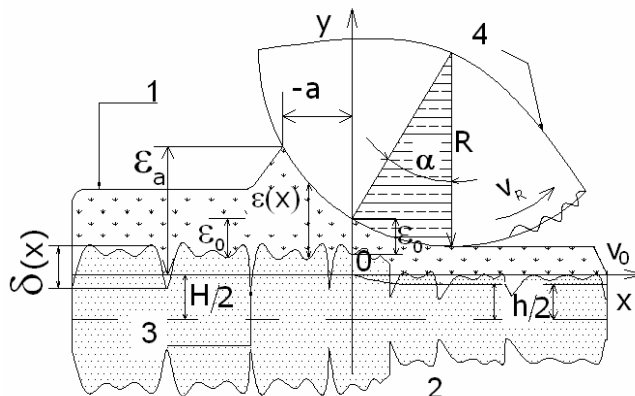


Figure 1: Geometry of the technological process

The geometry of lubrication contact is described by the expression (2), and the length of lubricating wedge is described by the expression (3), according to Figure 1:

$$\varepsilon(x) = \varepsilon_0 + R \left[\cos \alpha - \sqrt{1 - \left(\sin \alpha - \frac{x}{R} \right)^2} \right] \tag{2}$$

$$a = R \left[\sqrt{1 - \left(\cos \alpha - \frac{\varepsilon_a}{R} + \frac{\varepsilon_0}{R} \right)^2} - \sin \alpha \right] \tag{3}$$

The expression (2) has been transformed into Maclaurin series, and it is represented in the expression (4) to the fourth member, when gripping angles have a tendency to zero, i.e. for dressing and cold rolling processes with small gripping angles:

$$\varepsilon(x) = \varepsilon_0 - \alpha x + \frac{x^2}{2R} - \frac{\alpha x^3}{2R^2} + \frac{x^4}{8R^3} \tag{4}$$

The differential equation (1), which includes the effect of cross roughness of the strip or longitudinal roughness of the rollers, is developed into the following form [1-6], based on Figure 1:

$$\left\langle \frac{dp}{dx_0} \right\rangle = 6\mu(v_0 + v_R) \left[\left\langle \frac{1}{\varepsilon^2(x_0)} \right\rangle - \frac{\left\langle \frac{1}{\varepsilon^2_0} \right\rangle}{\left\langle \frac{1}{\varepsilon^3_0} \right\rangle} \left\langle \frac{1}{\varepsilon^3(x_0)} \right\rangle \right] \tag{5}$$

Random height of the lubricating layer $\delta(x)$, conditioned by the roughness of rollers and the strip, is added to the nominal height for smooth surfaces $\varepsilon(x)$:

$$\langle \varepsilon(x_0) \rangle = \varepsilon(x) + \delta(x) \tag{6}$$

This calculation can be completed only via numerical methods in mathematical applications. The authors used the Monte-Carlo numerical method, in the mathematica program.

In terms of theoretical research, the following "square wave" function was used for the model of cross-roughness of the strip, developed to the third member in the Fourier series:

$$\delta(x) = \frac{4}{\pi} \left(\sin x + \frac{1}{3} \sin 3x + \frac{1}{5} \sin 5x \right) R_z \tag{7}$$

$$\mu = \mu_0 \exp(\gamma * p) \tag{8}$$

Figure 2 includes a shift in the roughness of the strip for approximately $\pi/6$, or 30 degrees in relation to the rotating roughness of the rollers.

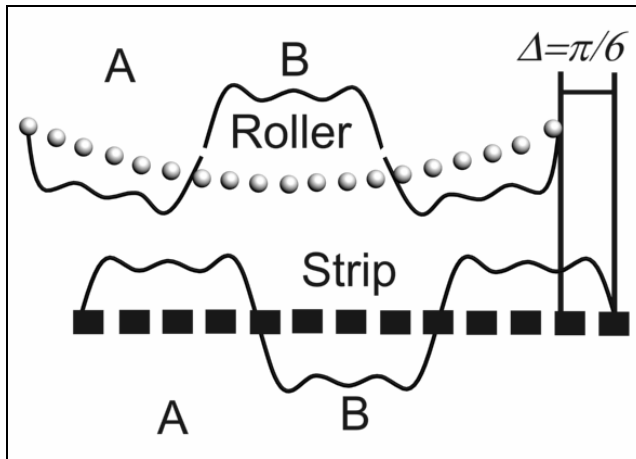


Figure 2: Cross-roughness of the strip and longitudinal roughness of the roller with phase shift

2. Solutions of the differential equation and the elaboration of results

Figure 3 provides a solution for the differential equation (5), when the roughness of the strip and the roller are congruent; i.e. when phase shift in Figure 2 is $\Delta \approx 0$. Interaction of positive ranges of roughness [A—A] lead to a clearly lower dosage of the lubricating layer in the area $L \approx \{1-33\}$, while interaction of negative ranges of roughness [B—B] results in better accumulation of the lubricant in inlet section of the deformation zone, and thus also in an increase of the thickness of the lubricating layer in the area $L \approx \{33-66\}$. Relative maximums of the lubricating layer are achieved in areas Ψ_0 and τ_0 . For the situation $L = A$, two lubricating islands are formed [1 and 2]. For the roughness class $S = 1$, the calculation of the lubricating layer is performed for ideally smooth surfaces, where, theoretically, the [A—B] ranges of roughness do not exist. In addition, the lubricating layer has an uninterrupted, continuous height. For $S = 11 \mu\text{m}$, roughness of surfaces points to the roughness class of $10 \mu\text{m}$. In ranges [A—A], we can observe discontinuous amorphous lubricating layers that appear at $S > 7$ microns. In this case, the lubricating layer is close to elastohydrodynamic lubrication, because the surfaces of the metal are in plastic condition with a constrained inflow of lubricant at $0 < L < A$. The height of the lubricating layer is in the range $7-8.5 \mu\text{m}$. For $S > 7$, the amorphous lubricating layer is consolidated into two lubricating "islands" [1 and 2], able to fulfill the lubrication function which is rendered more difficult at a small supporting profile of roughness in areas $L \approx 9$ and $L \approx 29$. The very formation and existence of these lubricating areas, which provide a solution to the differential equation (5), remains a phenomenon to be explained.

The effect of the mathematician Gibbs, as a phenomenon stemming from the development of Fourier series, is not acceptable – because the same occurrence would otherwise also have to be detected at [B—B], or for the range $33 < L < 66$, as a distinctive profile.

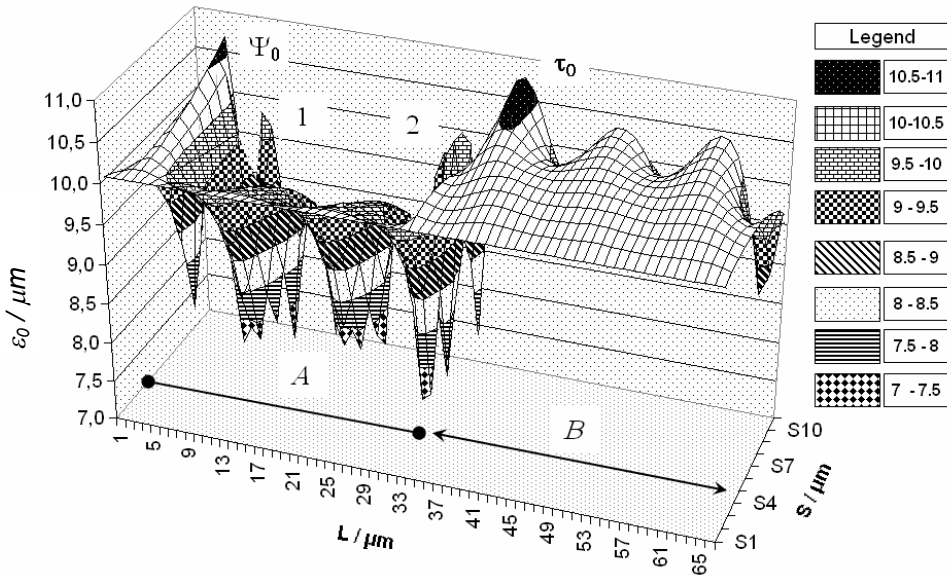


Figure 3: Solutions of differential equation when roughness of the rollers and roughness of the strip are congruent

Figure 4 contains solutions of the differential equation for the same conditions of the technological process, with phase shift of roughness of the strip as presented in Figure 2. Relative maximums of the lubricating layer, achieved in areas Ψ_0 i τ_0 , are shifted along the L axis proportionally to the phase shift of roughness in Figure 2. In this process, the division of lubricating islands occurred, with the following assumption:

$$1 - \frac{1\alpha}{1\beta} \quad \text{and} \quad 2 - \frac{2\alpha}{2\beta} \quad \text{or} \quad 1 - \frac{2\alpha}{1\beta} \quad 2 - \frac{1\alpha}{2\beta} \quad \text{Scheme (I)}$$

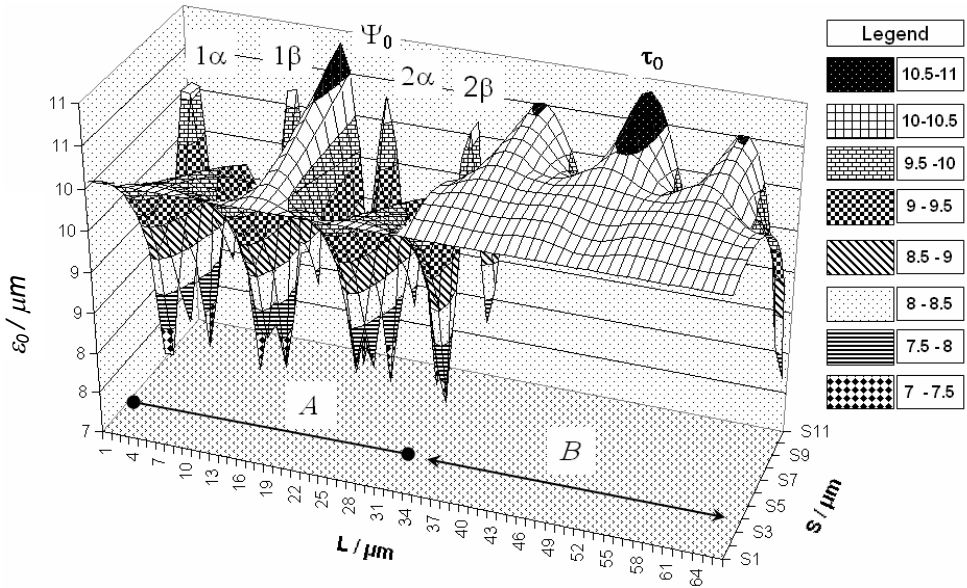


Figure 4: Solutions of differential equation for the case presented in Figure 2

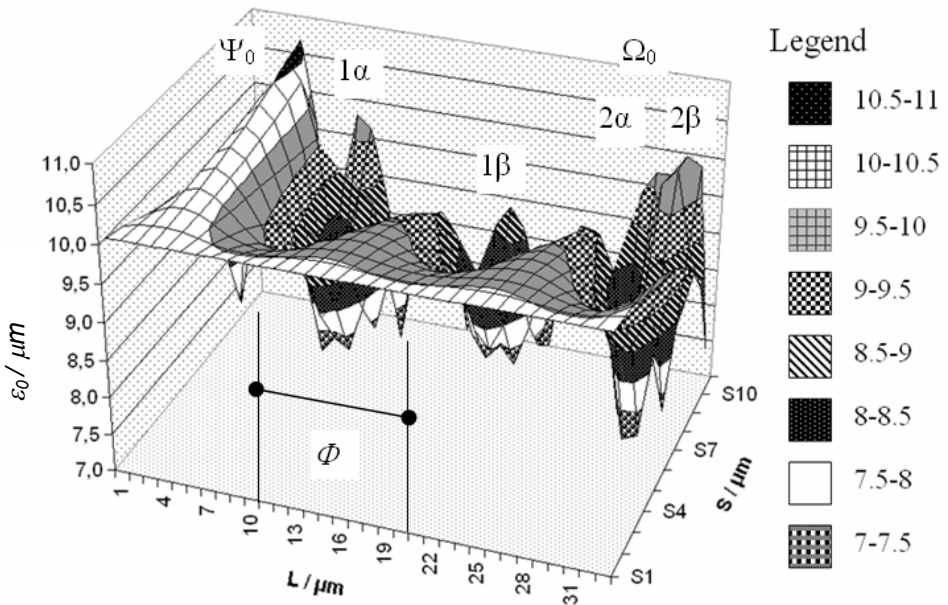


Figure 5: Refined approach to the negative range of roughness for conditions in Figure 3

It is difficult to determine – based on phase shift, and with the assumption of laminar flow of grease – which of these assumptions is more realistic. Due to this dilemma, the Monte-Carlo numerical method is repeated on the basis of a more precise zero approximation only on ranges of roughness [A—A]. Diagrammatic illustration in Figure 5 points to the fact that the first island of stability already split into two islands without phase shift $\Delta \approx 0$, while the other island Ω_0 is to be divided with certainty in a dynamic model. The prediction on how this will impact upon phase shift $\Delta \approx \pi/6$, in Figure 6, is now rendered even more difficult. What we can observe in Figure 6 with certainty is the fact that the lubricating layer will be distributed more uniformly, with phase shift along $L \approx \{ 1-33 \}$.

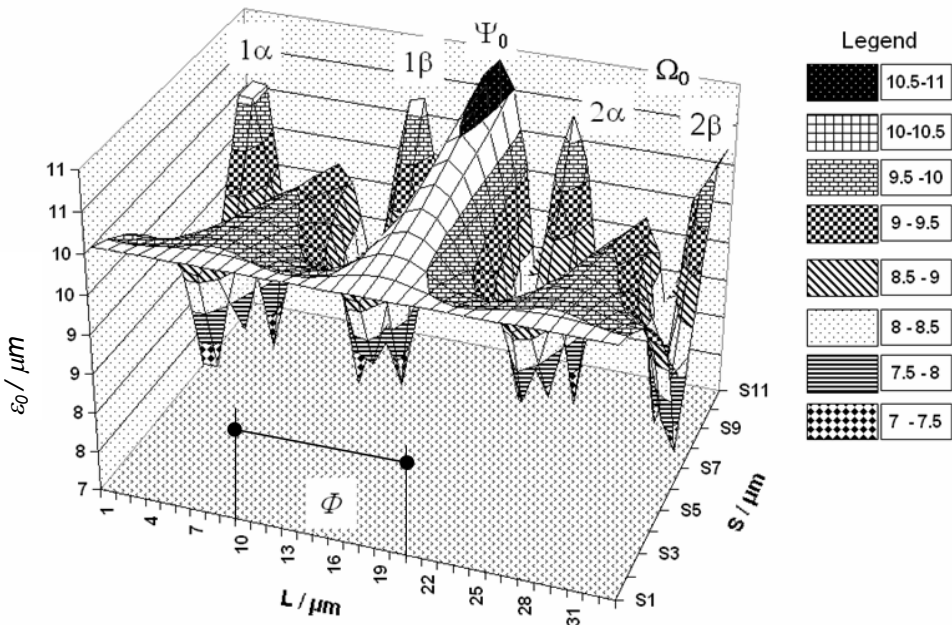


Figure 6: Refined approach to the negative range of roughness for phase shift.

In roughness class $S > 7 \mu\text{m}$, four lubricating areas have been created in amorphous lubricating layer in the range $1 < L < 33$, according to the scheme in Figure 2. A refined approach to the negative range of roughness, zoomed in Figure 5 in increment Φ , is represented in Figure 7. One can clearly notice that the first "island" became divided even without the phase shift of roughness. New repetition of calculation for $L=\Phi$ does not remove doubt regarding the appearance of the relative maximum of the lubricating layer, in Figure 8. Due to these dilemmas, we sought approximate analytical solutions that would confirm the Monte-Carlo numerical method for some simple cases, given the fact that the method pointed to important phenomena.

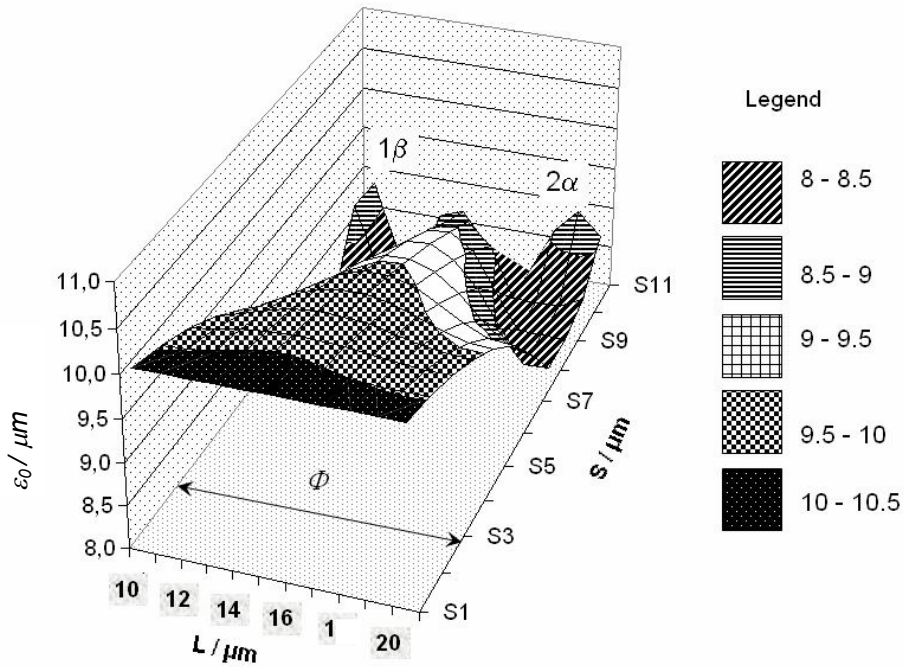


Figure 7: Clarification of the negative range of roughness in 3D illustration in Fig. 5

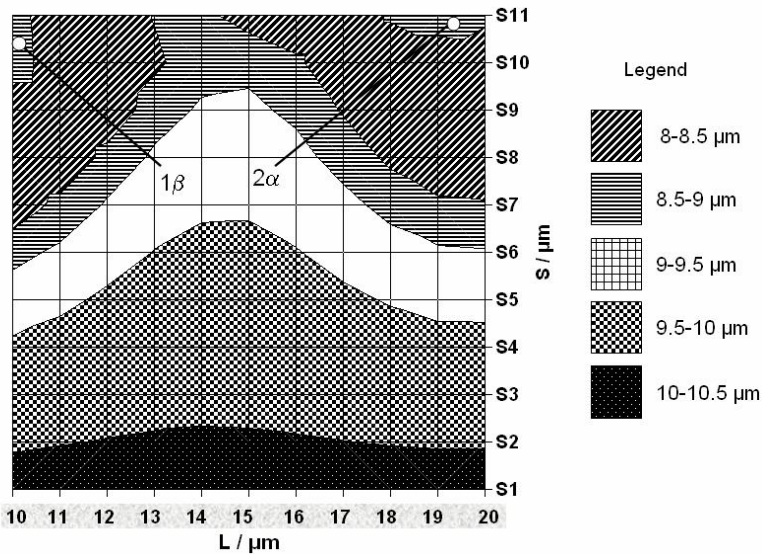


Figure 8: Contour plot of the negative range of roughness in area $L = \Phi$ in Fig. 7

This Figure, in the area $L=\Phi$, can not provide an indication as to which lubricating "islands" would be copied more naturally on Figure 6 according to the scheme (I).

4. Comparison of approximate analytical solutions with the numerical Monte-Carlo method in connection point

Numerical integration of the differential equation (6) was undertaken on the basis of reachable approximate analytical solutions, in order to arrive at practical implications. These analytical solutions are contained in formulas (9) and (11). Formula (9) represents the simplest form of analytical solution, which does not take into account the height of the lubricating layer on the strip, i.e. $\varepsilon_a \gg \varepsilon_0$. Formula (11) overcomes that shortcoming; however, it introduces a considerable degree of complexity.

$$315AR^3\alpha^7 - 168R^2\alpha^4 - 1824\delta^2 = 0$$

$$\varepsilon_0 = 0.5R\alpha^2 \dots A = \frac{1-\exp(-\eta p_0)}{6\mu\gamma(v_0+v_R)} \tag{9}$$

$$W1 = \left[\frac{4}{3\alpha^3 \cdot R} - 4 \cdot \frac{R^2}{3 \cdot \left[R \sqrt{1 - \left(\cos(\alpha) - \frac{\varepsilon_a}{R} + \frac{\varepsilon_0}{R} \right)^2} - R \cdot (\sin(\alpha) - \alpha) \right]^3} \right] \tag{10a}$$

$$W2 = \left[\frac{16}{7\alpha^7 \cdot R^3} - 16 \cdot \frac{R^4}{7 \left[R \sqrt{1 - \left(\cos(\alpha) - \frac{\varepsilon_a}{R} + \frac{\varepsilon_0}{R} \right)^2} - R \cdot (\sin(\alpha) - \alpha) \right]^7} \right] \tag{10b}$$

$$W3 = \frac{(\varepsilon_0)^3 + 3 \cdot \varepsilon_0 \cdot \delta^2}{(\varepsilon_0)^2 + 6 \cdot \delta^2} \tag{10c}$$

$$W4 = \left[\frac{8}{5\alpha^5 \cdot R^2} - 8 \cdot \frac{R^3}{5 \cdot \left[R \sqrt{1 - \left(\cos(\alpha) - \frac{\varepsilon_a}{R} + \frac{\varepsilon_0}{R} \right)^2} - R \cdot (\sin(\alpha) - \alpha) \right]^5} \right] \tag{10d}$$

$$W5 = \frac{32 \cdot R^5}{9 \cdot \left[R \sqrt{1 - \left(\cos(\alpha) - \frac{\varepsilon_a}{R} + \frac{\varepsilon_0}{R} \right)^2} - R \cdot (\sin(\alpha) - \alpha) \right]^9} \quad (10e)$$

$$W1+W2+W3 \cdot (W4 + W5) = 0 \quad (11)$$

This comparison has been prepared using a common example of theoretical research [5], and technological parameters are presented in the appendix. The results of calculations are presented in Table 1.

Table 1: Comparison of Monte-Carlo method in connection point with approximate analytical solutions

Parameter	Monte-Carlo (5)	Formula (11)	Formula (9)
	ε_0	ε_0	ε_0
x = 0 (starting profile of roughness), rollers are smooth $R_z = 1 \mu\text{m}$ $R_z \approx 6 \delta$ $\alpha = 0.00918759 \text{ rad}$ $A = 1965512 \text{ m}^{-1}$ $R = 0.35 \text{ m}$ $\varepsilon_a \gg \varepsilon_0$	$\varepsilon_0 = 14.772 \mu\text{m}$	$\varepsilon_0 = 14.771 \mu\text{m}$	$\varepsilon_0 = 14.721 \mu\text{m}$
x = 0 (starting profile of roughness) $R_z = 10 \mu\text{m}$ $R_z \approx 6 \delta$ $\alpha = 0.00840867 \text{ rad}$ $A = 3934525 \text{ m}^{-1}$ $R = 0.25 \text{ m}$ $\varepsilon_a = 0.001 \text{ m}$	$\varepsilon_0 = 8.755 \mu\text{m}$	$\varepsilon_0 = 8.776 \mu\text{m}$	$\varepsilon_0 = 8.838 \mu\text{m}$

According to the results in Table 1, the first example represents stable lubrication, while the second example represents friction between insufficiently moist surfaces, which is a frequent situation in practice.

The second example is close to the situation involving an amorphous lubricating layer, which means that we can conclude that the Monte-Carlo numerical method is interpreting mathematical modeling in a correct manner. However, the genesis of the formation of lubricating islands is not resolved by this; there are merely certain indications regarding the genesis.

5. Conclusion

The investigation of the roughness of surfaces in processes of strip dressing and cold rolling with lubricants has led to interesting perspectives. In the interaction of positive ranges of roughness of the rollers and the strip, the inflow of lubricant through inlet section of the deformation zone is rendered more difficult. In such a situation, areas insufficiently soaked in lubricant will occur naturally; however, areas that are soaked in lubricant may also occur partially. These subzones depend on uneven spots on the strip and the rollers, and the probability of their appearance may be linked with effects of the compressed burntout scale in the surface layer of the rolling metal, which also acts as a lubricant. During the phase shift of the roughness of the roller in relation to the roughness of the strip, compressed scale moves along the analyzed roughness profile, in proportion to phase shifts. In this process, there is a probability that "lubricating islands" would be divided into several stable islands, which, from a practical perspective, contributes to better lubrication of that particular profile of roughness where the lubricant is deficient during the interaction of positive ranges of roughness. It is worth pointing out that the congruence of the roughness of the roller and the roughness of the strip exists practically in milliseconds. We should also point out the fact that the speed of movement of the strip is different from the circumferential speed of rollers, which would not be possible under the assumption of gear interaction. The situation at hand leads with certainty to skidding of rolling metal between the rollers, as a phenomenon which is difficult to explain – and which certainly depends on various ways in which the roughness of the roller interacts with the roughness of the strip, as well as on other parameters of the technological process. By dividing subzones of "multilayered lubricating islands" with different phase shifts of roughness, the lubricant is more evenly dispensed on those parts of the strip where the inflow of lubricant is rendered more difficult, thus diminishing the vibration of the strip which is subjected to dressing, or which is rolled at high speeds. The investigation of this effect, which can be grasped from theoretical calculations outlined here, must be performed in several successive stages, by dividing the supporting profile of roughness into equidistances and by applying the Monte-Carlo method, because the offered analytical solutions are not relevant for such a dynamic approach. These analytical solutions can merely confirm the fact that they are accompanying the calculation well in only one part of strip roughness, when it is described as „homogenous roughness“ of an average uneven spot R_z .

For lubricant heights on strip above 1 mm, the proposed approximate analytical solutions can satisfy the mathematical calculation for the case of smooth rollers, using the approximate formula (9).

Taking into account the roughness of the strip and the roughness of the rollers, approximate analytical solutions are contained in formula (11). These solutions are valid for inlet section of the metal deformation zone in a wider range of gripping angles of cold rolling, with a certain isotropic homogenous roughness of the metal, providing a satisfactory match in comparison with the Monte-Carlo method.

List of symbols and clarification of figures

Symbol	Note (Dimensional analysis can be found in Table 2(<i>Appendix</i>))
A	Technological parameter according to the expression (11)
dp/dx	Pressure gradient in the lubricating layer along x axis
μ	Dynamic viscosity of lubricant for roller pressure
μ_0	Dynamic viscosity of lubricant for atmospheric pressure
γ	Piezocoefficient of lubricant viscosity
Exp	Euler's number (2.718...)
Sin x	Sinus function
P	Rolling pressure
P_0	Atmospheric pressure
v_0	Speed of strip movement (Figure 1)
v_R	Orbital velocity of a roll
Q	Expenditure of lubricant per perimeter of the strip
$\varepsilon(x)$	Lubricant height for smooth surfaces of rollers and the strip
x,y	Cartesian coordinates
ε_0	Lubricant height at inlet section of the deformation zone (calculated)
R	Roller radius
R_0	$R_0 = R \pm \delta(x)$
R_z	Average height of uneven spots
α	Pressure angle
-a	Active length of lubricating wedge (Figure 1)
ε_a	Lubricant height on the strip in front of the rollers
$\langle dp/dx_0 \rangle$	Pressure gradient in lubricating layer along x axis, for rough surfaces
$\langle \varepsilon(x_0) \rangle$	Random height of lubricating layer conditioned by the roughness of the rollers and the strip, in line with the Gaussian law of distribution in center (0,0)
$\langle \rangle$	Operator of mathematical hope (expectations)
$\delta(x)$	Random height of roughness of strip or rollers
$\varepsilon(x)$	Nominal height of lubricating layer when $R_z \rightarrow 0$ (smooth surfaces)
Sin (x)	Development of quadratic wave into Fourier series, formula (7)
H/2	Height of strip prior to deformation (dressing)
h/2	Height of strip at exit from deformation zone
Number 1	Lubricating layer
Number 2	Rough strip
Number 3	Strip roughness peaks in area $\delta(x)$

Number 4	Smooth roller, with added roughness at exit from deformation zone
Δ	Phase shift of roughness between the strip and the rollers
π	Angle measure in radians
A	Positive ranges of roughness of strip and roller
B	Negative ranges of roughness of strip and roller
Roller	Rough roller
Strip	Rough strip
Rollers	Rollers without roughness (referring to the nominal height of lubricant)
Squares	Strip without roughness (referring to the nominal height of lubricant)
Number 1	First island of stability of the lubricating layer
Number 2	Second island of stability of the lubricating layer
ε_0	Height of the lubricating layer at inlet section of the deformation zone (Figure 1)
Ψ_0	Stable lubricating horn in positive ranges of roughness when $\Delta \cong 0$ degrees
τ_0	Stable lubricating horn in negative ranges of roughness
L	Supporting profile of roughness along x axis
{ 1-33 }	Increment as per L_x axis
[A—A]	Clarification of the interaction of ranges of roughness for Figure 2
{ 1 i 2 }.	Reference to lubricating islands
S	Roughness classes as third dimension in 3D illustration
1α	Occurrence of a new island of stability for $\Delta \cong \pi/6$, by dividing the island by Number 1
1β	Hypothetical occurrence of a new island, with the same assumptions as in 1α
2α	Occurrence of a new island of stability for $\Delta \cong \pi/6$, by dividing the island by Number 2
2β	Hypothetical occurrence of a new island, with the same assumptions as in 2α
Ω_0	Metastable lubricating island, already prepared for division by phase shift
ϕ	Span of abscissa from 10 to 20 μm , which will be scrutinized closely
-----	All relevant symbols and clarifications are included
Legend	Lubricating layers in μm
$x = 0$	Roughness in center along abscissa of average uneven spot R_z – because function (7) cannot be built into approximate analytical solutions
[1-6]	Reference mark
Scheme (I)	Clarifies Figure 4
π	Transcendental number (3.141....)
$W_1 \rightarrow W_5$	Partial analytical solutions

References

1. D.Ćurčija, I. Mamuzić, *Mater. Tehnol.*, 43 (2009) 1, 23-30.
2. R. Boman, J.-P. Ponthot, *J. Mater. Process. Technol.*, 43 (2002) 405-411.
3. S. Thiruvardhelvan, M. J. Tan, *J. Mater. Process. Technol.*, 167 (2005) 2-3, 161-166.
4. O. P. Maksimenko, A. A. Semenča, *Plast. Deform. Met.*, 8 (2005) 447-452.
5. D.Ćurčija, I. Mamuzić, *Goriva i maziva*, 46 (2007) 1, 23-45.
6. P. Heyer, J. Lauger, *Lubr. Sci.*, 21 (2009) 7, 253-268.

Key words: cold rolling, strip dressing, lubrication, Reynolds equation, Monte-Carlo method.

Authors

Dušan Čurčija, Ilija Mamuzić

Croatian Metallurgical Society, Berislavićeva 6, 10000 Zagreb, Croatia

Marian Buršak, Tehnical Univerziteti of Košice, Slovakia

Jiri Klíber, Tehnical Univerziteti of Ostrava, Czech Republic

Received

30.09.2011.

Accepted

03.01.2012.

Appendix

Table 2: Common characteristics of lubricant for theoretical calculations

γ - piezocoefficient of viscosity	2.18E-7	Pa^{-1}
p - rolling pressure	20E6	Pa
v_R - orbital velocity of a roll	10	m/s
V_0 - strip velocity	6	m/s
R - radius of a roll	0.25 – 0.35	m
μ_0 - dynamical viscosity of lubricant $\mu = \mu_0 \exp(\gamma^* p_0)$ Baruss formula	0.024-0.048	Pas
α - pressure angle	0 – 0.02	rad
ε_a - lubricant height on a strip	0.001-0.00002	m
A - technological parameter	1965512 - 3934525	m^{-1}
$R_z \approx 6\delta$; (GOST-27189-S) ISO 1302-N	$R_z = (1 - 10) \mu m$	μm